Ecological Modelling 272 (2014) 160–174

Contents lists available at ScienceDirect

Ecological Modelling

journal homepage: www.elsevier.com/locate/ecolmodel

Numerical modelling and graph theory tools to study ecological connectivity in the Great Barrier Reef

Christopher J. Thomas[a,*], Jonathan Lambrechts[a], Eric Wolanski[c], Vincent A. Traag[d], Vincent D. Blondel[d], Eric Deleersnijder[a,e], Emmanuel Hanert[b]

[a] Université catholique de Louvain, Institute of Mechanics, Materials and Civil Engineering (iMMC), Avenue G. Lemaître 4-6, B-1348 Louvain-la-Neuve, Belgium
[b] Université catholique de Louvain, Earth and Life Institute (ELI), Croix du Sud 16, B-1348 Louvain-la-Neuve, Belgium
[c] James Cook University, TropWATER and School of Marine and Tropical Biology, James Cook Drive, Townsville, Queensland 4811, Australia
[d] Université catholique de Louvain, Institute of Information and Communication Technologies, Electronics and Applied Mathematics (ICTEAM), Avenue G. Lemaître 4-6, B-1348 Louvain-la-Neuve, Belgium
[e] Université catholique de Louvain, Earth and Life Institute (ELI), Georges Lemaître Centre for Earth and Climate Research (TECLIM), Place Louis Pasteur 3, B-1348 Louvain-la-Neuve, Belgium

ARTICLE INFO

Article history:
Received 26 March 2013
Received in revised form 2 October 2013
Accepted 4 October 2013

Keywords:
Larval dispersal
Marine connectivity
Coral
Great Barrier Reef
Graph theory
Community detection

ABSTRACT

The process of coral larval dispersal is important for coral reef ecosystems, but remains poorly understood and hard to gauge. Better knowledge of inter-reef connectivity patterns would be useful in enabling better management of coral reef waters however. By employing a spatially explicit numerical modelling approach, we simulate larval dispersal through the central section of the Great Barrier Reef (GBR), comprising over 1000 reefs, and identify spatial patterns in the inter-reef connectivity network using a community detection method from network science. This paper presents the modelling approach used and discusses the significance of the results.

Inter-reef connectivity networks were estimated for 4 different coral species, and significant differences between them were found. We show how we can partition reefs into clusters, or "communities", that are sparsely connected with each other, and therefore identify important barriers to larval dispersal. By fine-tuning a resolution parameter in the community detection method, we can find dispersal barriers of varying strength. Finally, we show that the average connectivity length scale varies significantly across the different reef communities, and suggest that this may have repercussions for the optimal placement of marine protected areas (MPAs) to maximise connectivity with surrounding reefs.

© 2013 Elsevier B.V. All rights reserved.

1. Introduction

For most types of coastal marine species, the process of larvae dispersing through the ocean prior to reaching adulthood – known as the pelagic larval phase – is vital in enabling population exchange between geographically separated sub-populations (Cowen and Sponaugle, 2009; Cowen et al., 2006). In coral reef ecosystems the pelagic larval phase takes on an added importance as marine life is predominantly concentrated onto reefs of varying size separated by open sea. Many species of reef fish never leave their home reef as adults (Jones et al., 2009), whilst coral is physically fixed to the reef surface and is thus unable to travel between reefs. It is therefore only during the pelagic larval phase that these species can spread to new reefs, repopulate damaged reef populations and maintain a healthy gene pool by exchanging larvae between separate sub-populations (Buston et al., 2012). Understanding how larvae disperse, where they can disperse to, and how resilient this process is to environmental change is essential to understanding the dynamics – and resilience – of coral reef ecosystems. Conservation strategies for coral reefs often involve the designation of Marine Protected Areas (MPAs) in which local anthropogenic interference is limited. In order for reefs in MPA networks to be effective in replenishing coral and reef fish populations in neighbouring reefs, the size and spacing of MPAs should account for the dispersal potential of marine species present in the region (Largier, 2003; Munday et al., 2009; Olds et al., 2012), which is not currently the case for most major coral reef ecosystems (Jones et al., 2009; Almany et al., 2009). Whilst some recent studies have proposed MPA designs which incorporate connectivity estimates to improve conservation performance, e.g. Mumby et al. (2011), Guizien et al. (2012), a major stumbling block so far has been a lack of location-specific knowledge of larval dispersion and

* Corresponding author. Tel.: +32 10478031.
E-mail address: christopher.thomas@uclouvain.be (C.J. Thomas).

0304-3800/$ – see front matter © 2013 Elsevier B.V. All rights reserved.
http://dx.doi.org/10.1016/j.ecolmodel.2013.10.002

connectivity patterns (Drew and Barber, 2012). Spatially explicit modelling studies such as the one presented in this article aim to fill this knowledge gap.

Larval dispersal remains very difficult to directly observe or measure, due to the small size of the larvae, the vastness of the ocean, and the fact that dispersion can occur over time-scales of days to weeks (Drew and Barber, 2012). Genetic tools can be used to measure the level of genetic connectivity between two given sub-populations, however these tools, whilst useful in quantifying present-day and historical connectivity, are by their nature unable to explain the processes driving the dispersion of larvae or to predict future trends (Palumbi, 2003), and are unable to provide spatially continuous detailed information over large regions. Numerical modelling tools can be used to fill this knowledge gap, both by providing large-scale estimates of present-day larval dispersion and connectivity patterns, and by showing how a change in physical or biological factors driving the dispersion process could alter inter-reef connectivity patterns (Werner et al., 2007).

The transport of larvae between separate reefs can be described in terms of "ecological" (or demographic) connectivity, which concerns the movement of individual larvae, or in terms of "genetic" connectivity, which concerns the exchange of genetic information. Ecological connectivity occurs over the time- and space-scales over which most larvae disperse (typically days to weeks and 0.1–100 km for coral) and is of primary interest for fisheries, reef management and MPA planning. Genetic connectivity on the other hand is a more complex process which plays out over many generations, with time- and space-scales spanning a greater range than ecological connectivity. For instance, the migration of just a few individuals per generation between two sub-populations can be enough to prevent genetic differences from developing, and can therefore represent a genetically significant level of connectivity (Cowen and Sponaugle, 2009; Leis et al., 2011), despite being ecologically insignificant. It is not a straightforward exercise to compare observed genetic connectivity with ecological connectivity predicted using large-scale numerical models as these models typically do not have enough precision to estimate transport down to ecologically insignificant (but still genetically significant) numbers of larvae, over time periods in the order of years.

In this paper we present a modelling approach to simulate larval dispersal down to reef-scale spatial resolution, and use this to study ecological connectivity in the region covering the central section of the Great Barrier Reef (GBR) in Australia, which includes roughly 1000 reefs. The GBR is a region with a particularly complex bathymetry and a correspondingly complex water circulation (Wolanski, 1994). Small-scale circulation at the reef-scale has been shown to interact significantly with large-scale circulation, for instance through the 'sticky water' effect (Wolanski and Spagnol, 2000; Wolanski et al., 2003; Andutta et al., 2012). In order to capture all major scales of motion, it is therefore necessary to resolve currents down to the reef scale: 100 m to 1 km. Present-day models of circulation in the GBR and other reef areas tend to have a horizontal resolution of 1–2 km however (e.g. Luick et al., 2007; Paris et al., 2007), too large to explicitly resolve flow at the lower range of larval dispersion length-scales, or even to capture many significant flow features in the reef-dense GBR. The use of nested structured grids is unfeasible in the GBR as the areas requiring enhanced resolution would be too numerous. In this study we instead use a finite element ocean model, SLIM,[1] to model water circulation in the GBR using an unstructured grid. This allows us to achieve reef-scale resolution around reefs at an acceptable computational cost (Lambrechts et al., 2008). We then employ an Individual Based Model (IBM) to simulate the dispersion and settling of coral larvae through the domain.

Large-scale spatially-explicit simulations such as this can produce a huge amount of data, so a set of tools is needed to interpret this output if we are to draw useful conclusions. A number of mathematical tools have been developed to study properties of networks, including biological and ecological networks of geographically separate, connected populations (Proulx et al., 2005). The use of these tools in studies of coral connectivity has so far been limited however. Treml et al. (2008) showed how graph theory can be used to investigate dispersal pathways and identify 'stepping-stone' islands linking distant populations and, more recently, Kininmonth et al. used a graph theoretical approach to explore the robustness and scale (Kininmonth et al., 2010b) of a reef network, as well as spatial clustering of connections (Kininmonth et al., 2010a). Nilsson Jacobi et al. (2012) used community detection tools to identify sub-populations in a network of marine habitats for generic sessile invertebrates in the Baltic Sea, and to infer the presence of dispersal barriers. They also investigated how many clusters contained MPAs, and concluded that MPAs were poorly distributed amongst the clusters.

In the present study we explore the use of a graph theoretical approach to identify spatial patterns in large-scale connectivity of coral larvae. We use a community detection method to identify clusters of reefs which are ecologically isolated from each other, and we partition the central section of the GBR into such clusters, known as "reef communities". Each reef community can be seen as a self-contained ecological sub-region, with little or no larvae exchanged with reefs in other communities. We establish maps delimiting separate reef communities in the GBR for 4 different species of coral, and find that significant inter-species differences exist in the size and shapes of the communities. These differences can be explained by variations in the biological characteristics of each species, and in particular their pre-competence periods. We also explore the differences in connectivity length scales across the different communities, and compare these to average MPA spacing. Such findings can potentially be used to inform the placement and spacing of MPAs to better take into account the different connectivity potential of larvae in each ecological sub-region.

This study has some parallels with Nilsson Jacobi et al. (2012), in which a similar graph theoretical approach to identify communities of generic sessile invertebrates in the Baltic Sea. Some differences of implementation between the two approaches are discussed in Section 2.3.2. No study that we are aware of has used these tools to compare the connectivity patterns of different marine species however, or to investigate whether dispersal patterns vary significantly in different sub-populations and how community-specific dispersal distances compare with MPA spacing.

2. Methods

The numerical modelling approach presented in this paper can be broadly divided into three stages: (1) modelling the hydrodynamics of the region, (2) simulating the transport of larvae, and (3) interpreting the model output. Each stage is now discussed, and a flow-chart summarising this process is presented in Fig. 2.

2.1. Resolving the hydrodynamics

2.1.1. Oceanographic model

Given the highly multi-scale nature of the water circulation in the GBR (as discussed in Section 1), it is important to use an ocean model able to cope with a large range of length scales. We used the finite element, unstructured-grid ocean model SLIM, in its

[1] Second-generation Louvain-la-Neuve Ice-ocean Model; see www.climate.be/slim for more information.

depth-integrated, barotropic version. SLIM is ideally suited to modelling water circulation in coastal and multi-scale regions due to its use of an unstructured grid, which allows the model resolution to be varied in space (Legrand et al., 2006). The grid used in this study is shown in Fig. 3. The element size varies from 400 m close to reefs and coastlines to 10 km in deeper 'open-sea' areas. This allows the model to explicitly capture small-scale circulation features through reef passages and around islands, which are known to have a significant impact on large-scale circulation (Wolanski and Spagnol, 2000), whilst using a coarser resolution in 'open-sea' areas where flow is known to be more uniform. This modelling approach allows computational resources to be focused to where they are needed most.

The SLIM model has already been shown to be capable of reproducing important small- and large-scale circulation features in the GBR by Lambrechts et al. (2008), and has been used and validated in various studies of the hydrodynamics and ecology of the GBR (e.g. Andutta et al., 2011, 2012; Hamann et al., 2011; Wolanski et al., 2013) and other coastal oceans and estuaries around the world (e.g. Sassi et al., 2011; de Brye et al., 2010).

Whilst this study focuses on larval dispersal in the central third of the GBR, from just north of Townsville (18.7° S) down to just south of Broad Sound (22.5° S), the grid covers the entire coastal ocean of the GBR from 11° S down to 25.5° S, but with a lower resolution in the northern and southern thirds, where larval dispersion is not simulated. This is to allow the boundary conditions to be imposed at the shelf break where the data are more reliable, and has very little effect on the computational cost of simulation due to the low resolution outside of the central third of the GBR.

2.1.2. Governing equations, forcings and paramaterisations

SLIM was used to solve the depth-integrated shallow water equations to calculate the water elevation η and the current velocity u:

$$\frac{\partial \eta}{\partial t} + \nabla \cdot (Hu) = 0 \tag{1}$$

$$\frac{\partial u}{\partial t} + (u\nabla)\cdot u = -fe_z \times u - g\nabla\eta - C_D|u|u + \frac{\tau}{\rho H} + \frac{1}{H}\nabla\cdot[H\nu(\nabla u)] \tag{2}$$

where H is the water column depth, f is the Coriolis factor, e_z is a unit vector pointing vertically upwards, C_D is the bottom stress coefficient, τ is the surface wind stress, g is the gravitational acceleration, ρ is the water density and ν is the horizontal eddy viscosity.

The model was set up in a similar way to that described by Lambrechts et al. (2008) and Andutta et al. (2011). The bathymetry data used were from the 100 m resolution dataset produced by Project 3DGBR (Beaman, 2010). The bottom stress coefficient is given as $C_D = g/(C^2H)$, with the Chezy coefficient $C = H^{1/6}/n$, and where the Manning coefficient used was $n = 2.5 \times 10^{-2}$ m$^{1/3}$ s^{-1}. This value was multiplied by 10 over shallow reefs to account for the increased roughness of reef surfaces. The positions of shallow reefs in the GBR were taken from the global distribution of coral reefs provided by the Great Barrier Reef Marine Park Authority (GBRMPA, 2007). The reefs are not considered emergent and have water over them at all times. Smagorinsky's paramaterisation was used to account for unresolved turbulent features and boundary layer effects around coastlines and islands, with horizontal kinematic eddy viscosity dependent on the local grid element size.

The external forcings applied to the model consisted of tides and residual currents at the open-sea boundaries and wind over the entire domain. Tidal forcing was applied at the boundaries using the OSU TOPEX/Poseidon Global Inverse Solution dataset (Egbert and Erofeeva, 2002), whilst wind data extracted from NCEP reanalysis was provided by NOAA/OAR/ESRL PSD (Kalnay et al., 1996). The wind stress acting on the sea surface was modelled using the paramaterisation proposed by Smith and Banke (1975). The effect of the East Australian Current was accounted for by imposing a constant residual flow into the domain at the boundary with the Coral Sea between 15.0° S and 17.6° S, and allowing this water to flow out through the southern and northern open-sea boundaries, following the same approach as Brinkman et al. (2001). The hydrodynamics were validated using observed oceanographic elevation and current data. This validation is presented and discussed in Appendix A.

2.2. Biophysical particle transport

The dispersal and settlement of larvae was modelled by considering millions of "virtual larvae" released into the domain as autonomous, buoyant, individual organisms, passively transported by the ocean currents and subject to some very simple biological processes. This is a type of individual based model (see Grimm et al., 2006 for an introduction to IBMs).

Transport of larvae was modelled using a random walk formulation of the 2D advection-diffusion equation[2] as outlined in Spagnol et al. (2001) and Hunter et al. (1993). The equations used were:

$$x_{n+1} = x_n + v_n\Delta t + \frac{R_n}{\sqrt{r}}\sqrt{2K\Delta t} \tag{3}$$

$$v_n = \left(u + \frac{K}{H}\nabla H + \nabla K\right)|_{x_n} \tag{4}$$

where x_n and x_{n+1} are the particle positions at time iterations n and $n+1$, respectively, Δt is the time difference between iterations, R_n is a horizontal vector of zero-mean random numbers with variance r, K is the horizontal diffusivity coefficient, H denotes water depth and u is the depth-averaged horizontal water velocity supplied by the ocean model. The time step used for the simulations in this study was set to $\Delta t = 90$ s. The horizontal diffusivity coefficient, K, was calculated using the paramaterisation presented in de Brye et al. (2010), which makes use of the formula of Okubo (1971) to introduce a dependence on the local hydrodynamic grid element size. This approach has been used in numerous studies of coastal seas and estuaries using multi-scale models (e.g. see Lambrechts et al., 2008; Andutta et al., 2011; de Brauwere et al., 2011; Hamann et al., 2011).

The advantages of modelling larval transport with an IBM are: (1) that we can know the start and end points of each larva released into the domain, and therefore directly measure the relative strength of larval exchange between every pair of reefs, and (2) that we can directly simulate age- and location-specific processes taking place on larvae (e.g. mortality, acquisition/loss of competence).

The particle-tracker used in this study also modelled two simple age-related biological processes taking place on the virtual larvae: mortality and acquisition/loss of competence, and these were modelled as described by Connolly and Baird (2010), with the mortality rate being either constant or taken from a Weibull distribution, depending on the species, and the onset and loss of competence modelled as a gradual process governed by fixed competence acquisition and loss rates. A larva was only considered capable of settling onto a reef whilst it was competent. The values of the parameters used in this study were based on the experimental observations of Connolly and Baird (2010).

The virtual larvae were released over all of the shallow-water reefs in the domain of interest. The number of larvae released over each reef was a proportional function of the reef's surface area, with

[2] $(\partial/\partial t)(Hc) + \nabla\cdot(uHc) = \nabla\cdot(HK\nabla c)$ where t is time, c is depth-integrated tracer concentration, H is water depth, u is the depth-averaged horizontal water velocity and K is the horizontal diffusivity coefficient.

greater numbers of larvae released over larger reefs. They were then tracked for the duration of the simulation. Once a larva had acquired competency, it was considered to settle onto the first reef it travelled over. As soon as a larva settled onto a reef it was immediately removed from the remainder of the simulation.

2.3. Extracting useful information

The output of the biophysical model is a large connectivity matrix whose elements give the strength of the connectivity between every pair of reefs in the domain, where the connectivity strength is at this point defined as the number of larvae released over the source reef which settled onto the sink reef. Thus the connectivity matrix encapsulates all of the relevant output from the particle tracking simulation.

Given the large number of reefs in the domain (over 1000), finding useful information from this matrix is a challenge in itself. The strategies employed can be broadly divided into two categories: statistical analysis and identifying spatial patterns. These will now be outlined in turn.

2.3.1. Statistical analysis

We can define some appropriate statistical quantities to characterise connectivity patterns within a given region. These can be used both to describe connectivity in the whole domain, and to compare the connectivity patterns seen in various well-chosen subregions.

- **Weighted connectivity length:** the characteristic length scale of connectivity between reefs. It is calculated as:

$$\frac{\sum_{\text{all connections}} \text{connection strength} \times \text{connection length}}{\sum_{\text{all connections}} \text{connection strength}} \tag{5}$$

  where the connection strength is given by the number of larvae released over the source reef that settled onto the sink reef, whilst the connection length is the radial distance between source and sink reefs.
- **Proportion of self-recruitment:** the proportion of connections for which the source and sink reefs are the same.
- **Average plume length:** the furthest distance from the source reef at which connections occur, averaged over all connections. This is an indication of how far away a typical reef's influence extends.

2.3.2. Identifying spatial patterns

Another way of characterising the connectivity of the reef network is to look for spatial patterns. It would be useful to identify clusters of reefs which are strongly connected to each other, but weakly connected to reefs outside of their cluster. By partitioning the GBR reef network into such clusters we can identify ecologically separate groups of reefs, and therefore infer the presence of barriers to larval dispersion between these groups.

We propose a graph theoretical approach to partition the GBR into reef clusters. The GBR can be cast as a directional, weighted graph by considering its reefs as nodes in the graph, and the transport of larvae between reefs as connections, or "edges", linking the nodes. The strength of each edge, known as its "weight", is given by the connection strength between the two nodes it connects (i.e. the number of larvae travelling from one node to the other), denoted by w_{ij} for an edge linking source reef i to sink reef j.

One particularity of this graph is that an edge linking two small reefs will have a much smaller weight than an edge linking two large reefs, as fewer larvae are released over the small reefs during the simulation. Connections between larger reefs then play a larger role than connections between smaller reefs, even where they only account for a small fraction of the total larvae released over the source reef. We mitigate this problem by normalising the edge weight by an appropriate quantity to make it "non-dimensional"; we chose to normalise the edge weight w_{ij} by the total number of larvae released at reef i (that have settled somewhere), denoted by s_i. We thus arrive at the normalised edge weight $A_{ij} = w_{ij}/s_i$. The net effect is to increase the importance of edges between small reefs, which would otherwise be dwarfed by the edges between the larger reefs.

The aim is then to partition this graph into a number of coherent clusters, known as communities, whose members are strongly connected with each other and weakly connected to the other nodes in the network. Many methods have been developed in recent years to partition a graph into communities (see Fortunato, 2010 for an extensive review). One of the most popular methods has been to optimise a quantity called "modularity", which is a measure of how strongly a graph is divided into clusters compared to a random graph (Newman and Girvan, 2004). A significant drawback of this method is that it suffers from a resolution limit (Fortunato, 2007), meaning that communities smaller than a certain scale (relative to the size of the graph) cannot be identified. In addition, the ecological significance of communities identified using modularity is not entirely clear, due to the comparison to a random graph.

We therefore chose to use a variant of modularity which does not suffer from these problems. Specifically, we employed the constant Potts model (CPM) developed by Traag et al. (2011) and Ronhovde and Nussinov (2010), which is based on the principle of comparing the density of edges within the communities to a constant resolution parameter, rather than to a random graph. More specifically, if we denote by S_c the set of nodes that belong to a community c, we can define by $e_{cd} = \sum_{i\in S_c, j\in S_d} A_{ij}$ the total weight between community c and d, and denote by n_c the total number of nodes in community c. CPM is then defined as

$$\mathcal{H} = -\sum_c e_{cc} - \gamma n_c^2, \tag{6}$$

where e_{cc} is simply the total weight inside community c, and γ is the user-defined resolution parameter. The minus sign is simply a matter of convention. The goal is to find a partition into communities for which $\mathcal{H}$ is minimal. The optimisation of $\mathcal{H}$ was carried out using a modified Louvain Method algorithm (Blondel et al., 2008), following the approach described in Traag et al. (2011). The CPM approach has also been used to study the community structure of a marine network by Nilsson Jacobi et al. (2012), who instead used a spectral based algorithm to optimise the objective function. A comparison of the performance of this algorithm with the Louvain Method algorithm is included in Appendix B. Both methods returned partitions of similar quality on benchmark networks, and returned similar partitions for a set of central GBR connectivity networks.

CPM has two principal advantages (Traag et al., 2011). Firstly, it doesn't suffer from a resolution limit. Hence, there is no theoretical smallest or largest scale beyond which it is unable to identify communities. Secondly, the communities have a natural interpretation, which is twofold. First, in an optimal partition, each community has an internal connectivity of at least γ, i.e. $e_{cc}/n_c^2 \geq \gamma$. Second, two communities in an optimal partition are separated by a connectivity of at most γ, i.e. $e_{cd}/n_c n_d \leq \gamma$. In other words, the communities identified by the algorithm should have the two following properties:

Inner connectivity	The average connection strength between members of the same community is greater than γ.
External connectivity	The average connection strength between any two reefs in different communities is less than γ.

This approach allows us to detect reef communities at different spatial scales. If we use a low value of γ, the connectivity between any two communities will be small (i.e. we have nearly impermeable community boundaries), but the internal connectivity may also be low and the size of the communities will tend to be large. If instead we use a higher value of γ, the connectivity between any two communities may be higher, but the internal connectivity will also be higher and communities will tend to be smaller and boundaries more permeable. The γ value is therefore an indication of how much inter- and intra-community connectivity there is. This concept is illustrated in Fig. 4.

This naturally leads to the question of how to find the "optimal" value of the resolution parameter, γ. In reality there is no "optimal" value: the size of the value used clearly depends on what question we want to answer. Imposing a small value of γ will partition the GBR into a small number of large, weakly connected communities. This will allow us to identify the most ecologically isolated reef communities, and will therefore allow us to find the strongest boundaries to larval dispersion in the GBR. Imposing a higher value of γ will allow us to identify smaller communities which may exist within the boundaries of the larger communities, and thus identify more localised or weaker barriers to dispersion.

A sensitivity analysis is carried out to identify how (1) the number of communities and (2) the percentage of inter-community connectivity vary over a range of γ values. An example of such a sensitivity analysis, showing the variation of the proportion of inter-community connectivity with γ, is shown in Fig. 5. This figure illustrates how the inter-community connectivity increases in distinct steps as γ is increased. Each jump in the curve generally corresponds to a significant change in the community partitions identified by the algorithm. Between two jumps there are plateaux of relatively stable connectivity over some interval $[\gamma_1, \gamma_2]$. Larger plateaux then correspond to especially pertinent partitions, since the external connectivity will in general be lower than γ_1 whilst the internal connectivity will be higher than γ_2. We then choose a selection of values of γ for which these variables are relatively stable, indicated by the asterisks in Fig. 5, and compare the community configurations obtained using each of these values.

Since boundaries to larval dispersion generally arise due to topographic features or between areas with distinct water circulation patterns, we can reasonably expect that the characteristics of larval dispersion in each community may be distinct from each other. We therefore calculate the statistical quantities defined in Section 2.3.1 for each reef community and compare them, to see if there is a significant variation in connectivity length-scales in the different communities. If, for a given value of γ, all of the communities identified have similar connectivity length-scales then we will generally choose to ignore that particular configuration, as it does not identify communities with significantly different connectivity patterns. Ultimately the goal is to identify the configurations which partition reefs into communities with physically distinct dispersal patterns.

3. Results and discussion

Virtual larvae were released over all reefs in an area encompassing the central GBR – roughly one-third of the GBR's total area. Larval dispersion was simulated for 4 different species of broadcast spawning larvae for which mortality and settling data were readily available: *Goniastrea retiformis*, *Acropora gemmifera*, *Platygyra daedalea* and *Acropora millepora*. All four species are known to be present in the GBR. The oceanographic forcings used were for the period of December 2007, corresponding to a typical coral mass spawning period, and the positions of the larvae were tracked for 4 weeks. After this period the proportion of larvae still alive was very small (<4% for all species). Whilst variations in oceanographic conditions between successive annual spawning seasons may modify larval dispersal patterns year-on-year, we chose to focus on one single season, as the scope of this paper is not to provide yearly estimates of dispersal patterns but rather to develop tools which can be used to study connectivity patterns for any given spawning season.

3.1. Dispersal statistics

The graph showing connection strength against distance for the different species studied is shown in Fig. 7. Inter-species differences in dispersion potential are clearly visible. Table 1, showing the global connectivity statistics, provides some additional detail. The proportion of larvae self-recruiting varies significantly between species, from 55% for *G. retiformis* to 18–19% for *A. gemmifera* and *P. daedalea* and down to only 13% for *A. millepora*. This difference is explained by the fact that the latter three species have much longer average pre-competency periods than G. retiformis: their larvae typically start to acquire competence after 3–4 days, whereas larvae of *G. retiformis* start to become competent immediately, and so are more likely to settle close to their release site. This is shown in Fig. 6, which shows the proportion of larvae alive and competent during the simulations. The later this curve peaks, the longer the average pre-competence periods, and so the longer the period during which the larvae can be advected and diffused away from their natal reef prior to settlement.

The typical length-scales over which most connectivity occurs tell a similar story to the self-recruitment statistics: *G. retiformis* larvae settle closer to their natal reef than the other species, with an average connectivity length of 6 km, whilst *A. millepora* tend to settle furthest from their natal reef, with an average connectivity length of 31 km. Long-distance connectivity (where long-distance is here defined as >100 km) is marginal in ecological terms for all 3 coral species, though not entirely insignificant for A. gemmifera, *P. daedalea* and *A. millepora*. Finally, the average plume lengths indicate that we would expect to see some minimal larval exchange at distances of over 80–130 km from the source reef, depending on the species.

3.2. Spatial patterns for G. retiformis

The community detection method described in Section 2.3.2 was used to partition the reefs into reef communities. For each species a set of different possible partitioning arrangements was generated by varying the value of the resolution parameter, γ, through a given range. A selection of different partitioning arrangements for the species *G. retiformis* is given in Fig. 8, showing different partitioning arrangements obtained using a low, a medium and a high value of γ. These correspond to arrangements with low, medium and high levels of inter-community connectivity respectively. We will focus our description on *G. retiformis* for now, as the effect of varying γ has a similar effect for the other species. We will subsequently compare equivalent community configurations obtained for different species.

The partitioning arrangement obtained with the lower value of γ, shown in Fig. 8a, exhibits a very low level of inter-community connectivity – just 0.001%. In other words only 1 in every 100,000 settled larvae settled outside of their reef community, so broadly speaking the number of larvae crossing community boundaries is ecologically insignificant. We can see that the reefs around the Whitsunday Islands have been grouped together in the same community as the offshore reefs, as the level of transport between the two areas is not entirely insignificant. Perhaps surprisingly, the group of coastal reefs just south of the Whitsunday Islands is in a separate reef community, implying that the model predicted negligible levels of transport between the two communities, despite their geographic proximity. This is

Table 1
Summary of global connectivity characteristics for each species of coral after a 4-week simulation of larval dispersal. For an explanation of each quantity see Section 2.3.1. Average plume length is shown with its standard deviation.

Coral species	Self-recruitment (%)	Weighted connectivity length (km)	Long-distance connectivity (%)	Average plume length (km)
G. retiformis	55	6	0.3	80 ± 60
P. daedalea	19	20	1.6	117 ± 69
A. gemmifera	18	20	1.2	112 ± 68
A. millepora	13	31	5.0	131 ± 73

an indication that the "isolation-by-distance" method for estimating inter-reef connectivity is not always reliable in areas with complex topography and flow patterns, at least at small scales. We can also see that the average length of the connections within each community, also shown on the diagram, vary significantly from one community to the next. This suggests that larval dispersion dynamics are different in each community.

Fig. 8b shows a partitioning arrangement if we increase the value of the resolution parameter such that inter-community connectivity now accounts for 1% of all connections. The reef communities are therefore still ecologically isolated units, as only 1 in every 100 settled larvae crosses a community boundary, but these boundaries can now be considered to be slightly less rigid. Looking at this partitioning arrangement, we can see that many smaller-scale community structures exist within the large-scale community structure shown in Fig. 8a. In particular, the large block of offshore reefs has been separated from the Whitsunday Islands community, meaning that the "barrier" to dispersal between the Whitsunday Islands group and the offshore reefs (which physically corresponds to a channel of southward-flowing open water), whilst not as significant as the "barrier" between the Whitsunday Islands and the coastal reefs south of them seen in Fig. 8a, is still more significant than any "barrier" within the Whitsunday Islands themselves, since these are still a whole community. It is also revealing that the difference in the weighted connectivity lengths in the offshore reef communities and in the Whitsunday Islands community is much more significant than any difference seen in Fig. 8a. This suggests that the different reef communities identified with this "medium" value of γ, and shown in Fig. 8b, have much more distinctive dispersal dynamics.

A partitioning arrangement obtained using a higher value of γ, in which 4% of connectivity crosses community boundaries, is shown in Fig. 8c. This figure reveals a more complex structure of communities in both the offshore group of reefs and in the Whitsunday Islands group. Most offshore reef communities are inclined along the longshore axis suggesting that reefs are better connected along this axis rather than along the cross-shelf axis. This is because the net currents act in the south-eastward longshore direction. With a couple of exceptions, most of the offshore reef communities have very similar average connectivity lengths. This suggests that there are no major differences in the dispersal dynamics amongst the offshore reefs.

It is more interesting however to look at the reefs around the Whitsunday Islands. At the higher γ, they have been split into three separate communities: one "coastal" community of nearshore reefs, with a very small weighted connectivity length (3 km), another "middle" community of reefs with a much greater weighted connectivity length of 22 km, suggesting that some larvae from this community settle far away from their natal reef, and finally another "external" community of reefs on the outer, eastward-facing side of the Whitsunday Islands. Somewhat surprisingly, these reefs also have a small weighted connectivity length – only 3 km – suggesting that either these reefs are more sheltered than those in the "middle" community, or else simply that most of the larvae released here are lost to sea and don't find any reefs to settle onto far away.

We can gain an insight into the physical processes causing this difference by looking at the effects of the water circulation on transport around the Whitsunday Islands. Fig. 9 shows the simulated dispersal of particles released at 5 different carefully chosen sites around the Whitsunday Islands after 3.5 days and after 1 week. In the simulation used to create these figures, the particles underwent no mortality or settling processes, so we can use these images purely as a guide to potential dispersal rather than as a prediction of real dispersal for a given species. We should note that in the species-specific simulations, after 3.5 days 93% of *G. retiformis* had settled onto a reef, whilst after 7 days this number was 97%. This means that very few *G. retiformis* larvae would have dispersed further from their release point than shown in both figures. It is clear from these images that particles released on the eastward-facing external side of the Islands tend to stay closer to their release point and are advected to the open sea where there are no reefs, whilst particles released in middle section tend to disperse further away and pass through other reef-dense areas. Furthermore, there is little mixing between particles released on either side. This explains why the two sides are placed in different communities for *G. retiformis*, and why the connectivity length scales are so different in these communities.

In summary, Fig. 8a–c shows different possible partitioning arrangements for *G. retiformis*, each of which gives us a different set of information. The question is which is the most useful? We suggest that all three are useful in that they complement each other, and provide us with information about the network over different length scales. Fig. 8a suggests that as a first large-scale approximation we should at least treat the coastal reefs south of the Whitsunday Islands, and the reefs in Broad Sound, separately from the other reefs in the domain. Fig. 8b shows that, in addition to this clear separation, there are also very significant differences on a smaller scale between the dispersal patterns of larvae released around the Whitsunday Islands and those released on the offshore reefs, and finally Fig. 8c shows that the Whitsunday Island reefs can themselves be subdivided into three different areas with distinct patterns of larval dispersion. Depending on the scale at which we want to look at the system, we should select a value of gamma which highlights the information relevant for that scale.

3.3. Spatial patterns for all species

Fig. 10 shows partitioning arrangements for all four species studied, where the percentage of inter-reef connectivity is fixed at around 4% – high enough to see the smaller reef communities but low enough to be ecologically marginal or insignificant. This figure shows that the species with the highest dispersal potentials – primarily *A. millepora* – form the largest communities, whilst *G. retiformis* form the smallest communities. This is because *A. millepora* larvae take longer to acquire competence and thus tend to travel further from their natal reef before settling (as reported in Table 1); they are therefore more capable of overcoming physical barriers to dispersal than other species.

Despite these differences in community size however, we can still see some patterns recurring for all of the species in the central GBR. For instance, the dispersal boundary between the

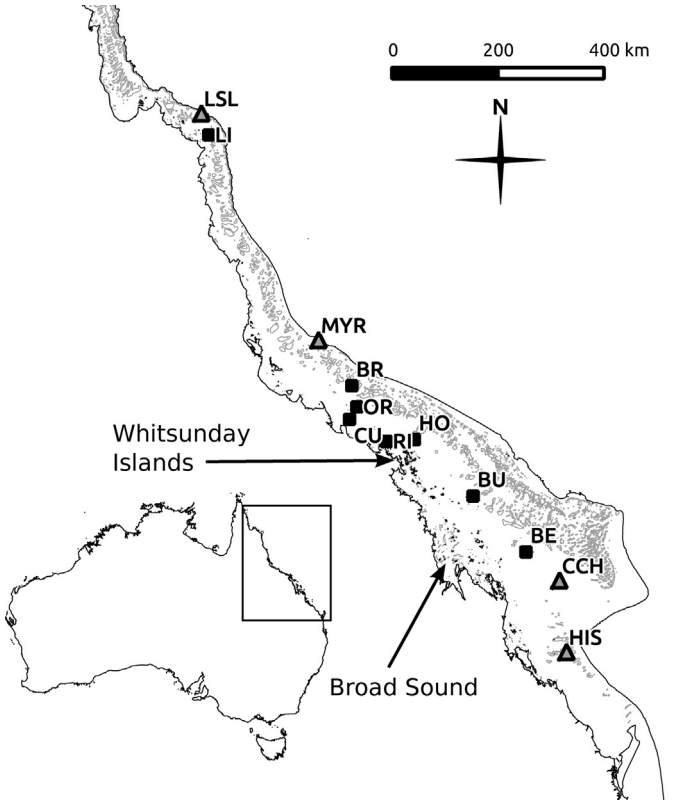

Fig. 1. Map of the GBR topography. The coastline is shown to the left, the 200 m-isobath to the right, and reefs are shaded in grey. Triangles show positions of moorings used to validate elevation, squares represent moorings used to validate currents. *Legend*: LSL: Lizard Island Slope, MYR: Myrmidon Reef, CCH: Capricorn Channel, HIS: Heron Island South, LI: Lizard Island, BR: Bowden Reef, OR: Old Reef, CU: Cape Upstart, RI: Rattray Island, HO: Hook, BU: Bushy, BE: Bell.

Whitsunday Islands and the offshore reefs is always present. The boundary between the Whitsunday Islands and the coastal reefs just south of them is also present for all species, despite their geographical proximity. The typical connectivity length scales also

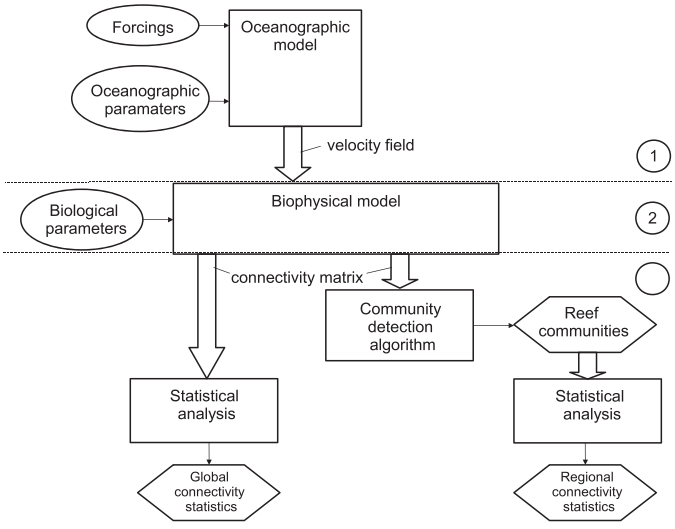

Fig. 2. Flow chart summarising the connectivity modelling process. Input parameters obtained from observations are shown in ovals, modelling stages are shown in rectangles and outputs are shown in hexagons. Thick arrows represent model outputs subsequently used as inputs for the next modelling stage. Circled numbers indicate the modelling stages: 1: simulating the hydrodynamics, 2: simulating larval dispersion, 3: extracting useful information.

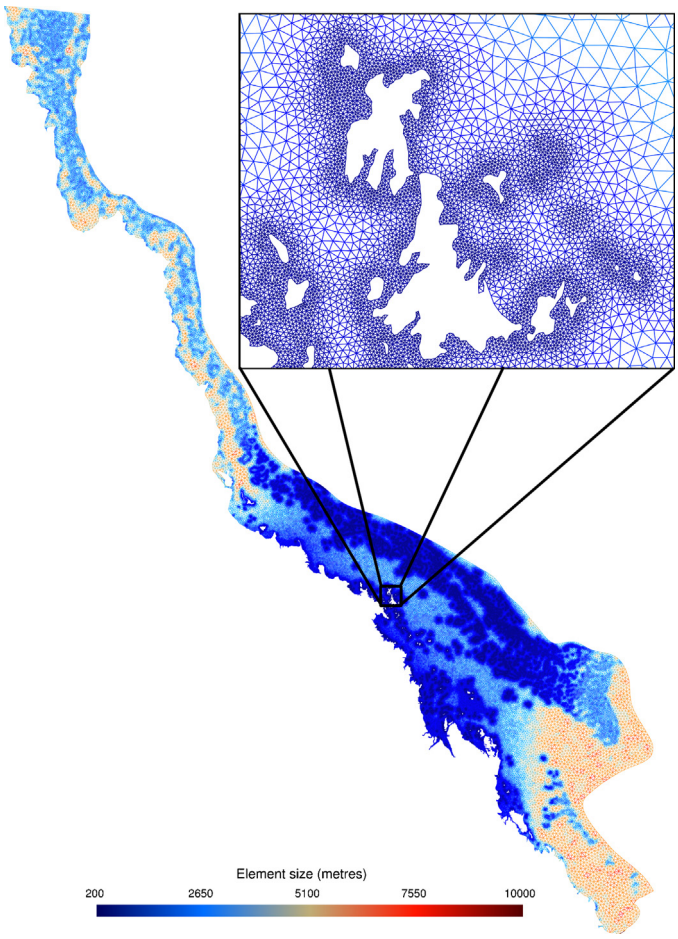

Fig. 3. The oceanographic grid used for simulations. The grid is colour-coded by the local characteristic element size – smaller elements are shown in blue and larger elements are shown in red. The element size is a function of water depth and distance to the nearest reef. In addition, the element size is further reduced in the central GBR region. The grid contains roughly 500,000 triangular elements. The western boundary is the North Queensland coastline whilst the northern, eastern and southern boundaries are with the open sea. The box shows grid detail around the Whitsunday Islands. (For interpretation of the references to color in this figure legend, the reader is referred to the web version of the article.)

vary significantly from one community to another, and tend to be smaller for nearshore reef communities and larger for offshore communities. This suggests that community boundaries often coincide with boundaries between areas with different larval dispersal dynamics.

Fig. 10 also reports the average distance between the nearest neighbouring MPAs (GBRMPA-designated "green zones", or no-take areas) in every community containing 2 or more MPAs. These figures show that MPA spacing does to some extent follow the same trends as larval dispersal distances; in nearshore areas MPAs tend to be closer together, whilst they tend to be further apart in offshore reef areas. This is positive for promoting connectivity between separate MPAs, as larvae tend to settle closer to their natal reef in nearshore areas. One notable exception is in Broad Sound, where MPA spacing is larger than in other nearshore areas, yet larval dispersal distances remain small.

For the three species which disperse the furthest (*A. millepora*, *P. daedalea* and *A. gemmifera*), the dispersal distances are not too dissimilar to the MPA spacing,[3] suggesting that many MPAs may

[3] It is important to bear in mind that the weighted connectivity length reported is only showing the average distance travelled by larvae; thus some larvae will be travelling further than this, as shown in Fig. 7.

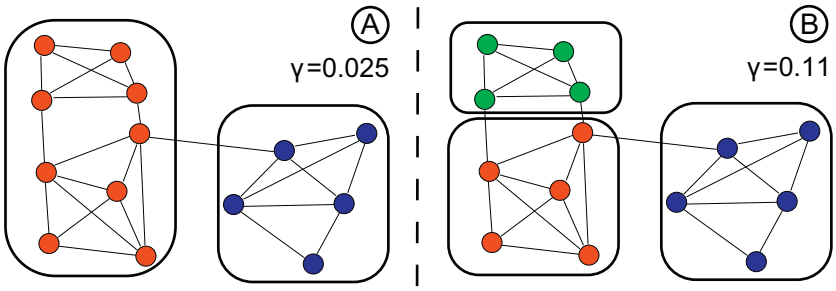

Fig. 4. Example illustrating the role of the resolution parameter γ in the community detection method. Diagrams A (left) and B (right) show two identical graphs, with the circles representing nodes and the lines between them representing connections. These connections all have equal weight. Both graphs have been partitioned using the community detection algorithm described in Section 2.3.2, and the thick lines and colour-coding demarcate the communities. The graph in diagram A was partitioned with the resolution parameter, $\gamma = 0.025$, whilst the graph in diagram B was partitioned using $\gamma = 0.11$. Using a lower value of gamma imposes a stronger constraint on the maximum connectivity allowed between any two communities, and so results in fewer communities being detected.

be ecologically connected to their neighbours. It is notable that some reef communities do not even contain 2 MPAs, however, particularly the smaller communities. For *G. retiformis*, whose larvae disperse over smaller distances, typical dispersal distances tend to be much smaller than average MPA spacing, and most communities do not contain 2 MPAs. This suggests that the level of connectivity between MPAs is likely to be very species-dependent.

4. Conclusions

The process of larvae dispersing through the Great Barrier Reef is controlled by a multitude of factors, both physical (relating to marine transport) and biological (relating to the behaviour and development rate of the larvae). By using an unstructured-grid ocean model as a tool to simulate the ocean circulation in the GBR, we have been able to resolve flow from the large-scale down to the reef-scale, an essential pre-requisite for modelling larval dispersion in the GBR, as this can occur on length-scales ranging from hundreds of metres to hundreds of kilometres.

Using a relatively simple biological model, we have made large-scale predictions of larval dispersal using a small number of biological parameters, following the best available present knowledge of larval mortality and development rates as found by Connolly and Baird (2010). Whilst this simple model of larvae as passive massless objects is deemed sufficient to model the transport of coral larvae, an increase in model complexity would be essential for modelling fish larvae instead, in particular to account for their ability to directionally swim (see Gerlach et al., 2007; Fisher and Bellwood, 2003; Vermeij et al., 2010). This is an area we plan to study in the future.

We have used a novel strategy to extract useful information from the connectivity matrix by employing a graph theoretical approach to identify ecologically separate reef communities. We have calculated connectivity characteristics separately for each reef community, and we have shown that the dispersal potential of larvae in different communities can vary significantly. We have provided estimates of dispersal potential in each community for 4 different coral species for a given spawning season, and we have shown that there are significant differences in the dispersal patterns and potentials between these 4 species. We have also compared these community-specific dispersal distances to the average spacing between neighbouring no-take MPAs in each community, and found that connectivity between MPAs is species-specific, and that MPA spacing does not always reflect the spatial patterns seen in larval dispersal distances.

In order to translate this approach into practical advice on MPA placement, the next step should be to quantify the effects of annual

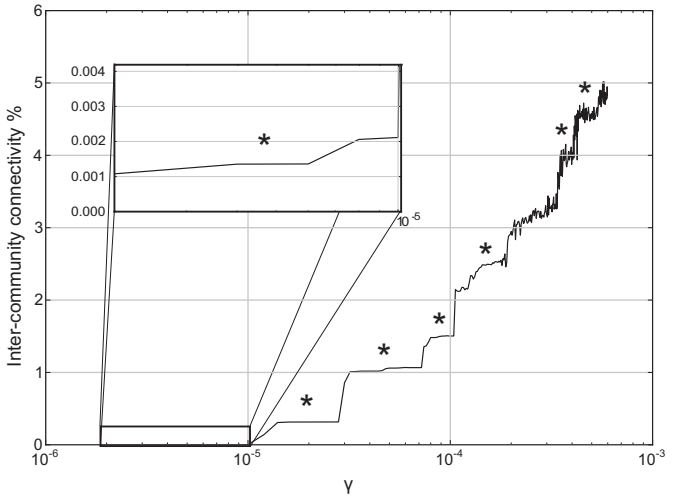

Fig. 5. The percentage of connectivity crossing community boundaries as a function of the resolution parameter, γ for *G. retiformis* coral larvae. The jumps correspond to significant changes in the partitioning configuration. The asterisks identify 'stable' partitioning configurations. The scale is logarithmic in x, as a given interval of γ at the lower end of the scale will be more significant, proportional to the local value of γ, than at the higher end of the scale.

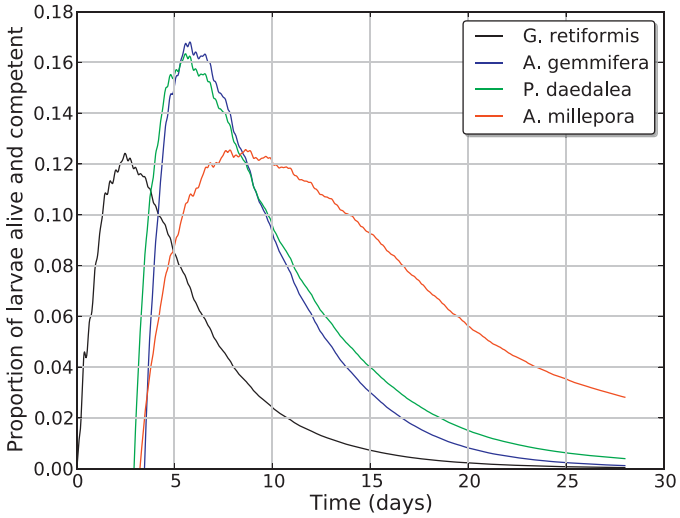

Fig. 6. Graph showing the proportion of larvae that are alive and competent to settle for each species during the simulation. A greater proportion of *G. retiformis* larvae are alive and competent in the days immediately after release than any of the other species, which explains their higher self-recruitment rate and lower weighted connectivity length.

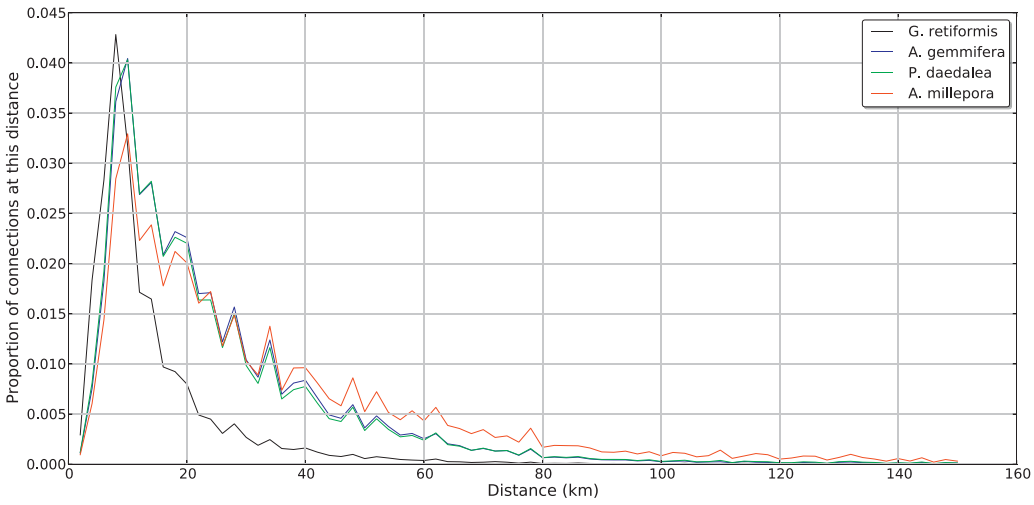

Fig. 7. Graph showing the connection strength against distance for larvae of 4 different species of coral, after a 4-week simulation. The distance is measured as radial distance between source and sink reefs. The *x*-axis (distance) is cut at 150 km. Self-recruitment is not shown in this graph, however it is used to calculate all other connectivity length-scale statistics.

variation of larval dispersion patterns on the shape and positions of communities, and on the connectivity characteristics of each community for a given species. Results obtained by Kininmonth et al. (2010b) suggest that the dispersal network structure of the GBR may undergo significant annual changes, but that stronger connections are highly likely to remain in place, at least for the stretch of the GBR considered in their study. It would also be useful to consider a much larger number of different coral species, as it is known that significant inter-species variations in connectivity can exist (Drew and Barber, 2012), though this may be hampered

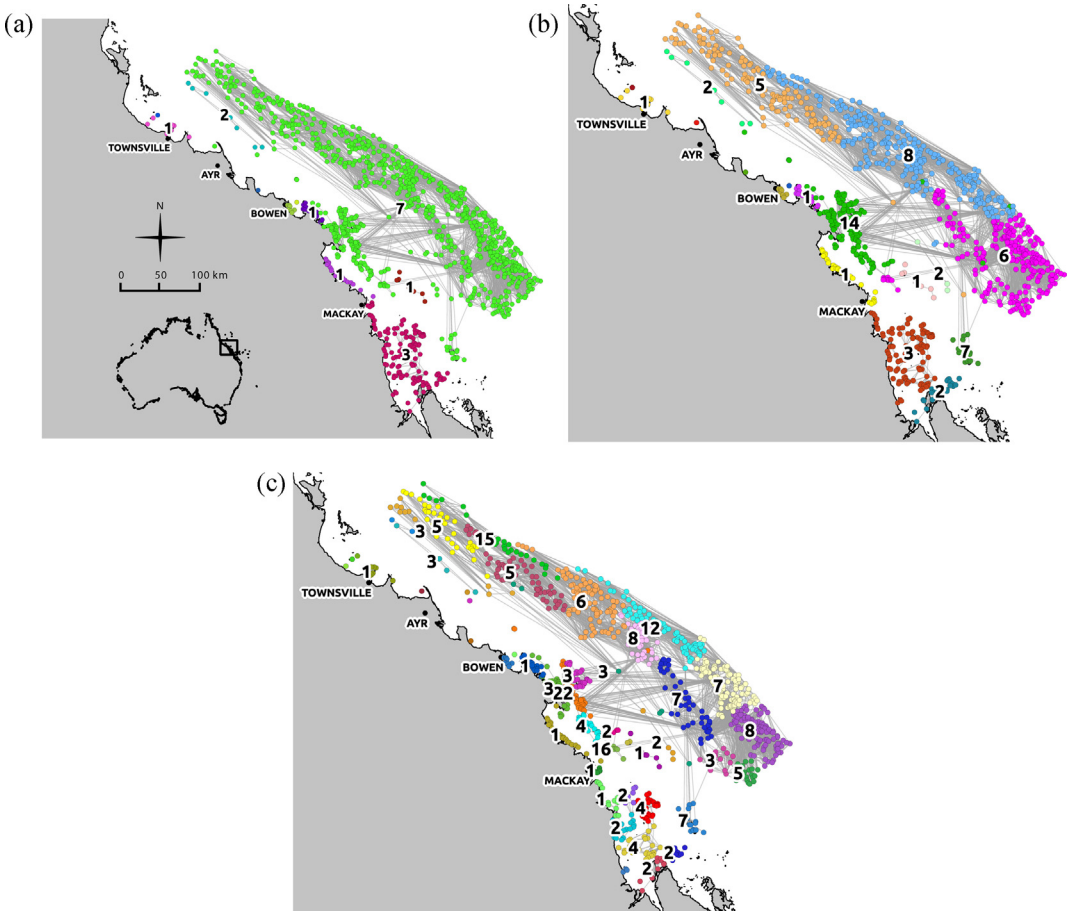

Fig. 8. Different reef community configurations for *G. retiformis* larvae. These different partitions were obtained by increasing the resolution parameter in the community detection method from a low value (a) to a high value (c). The numbers in the white circles show the average weighted connectivity length in each community, in kilometres. Connections between reefs are shown in light grey for illustrative purposes, with the weaker connections filtered out. (a) *G. retiformis*; inter-community connectivity: 0.001%. (b) *G. retiformis*; inter-community connectivity: 1%. (c) *G. retiformis*; inter-community connectivity: 4%.

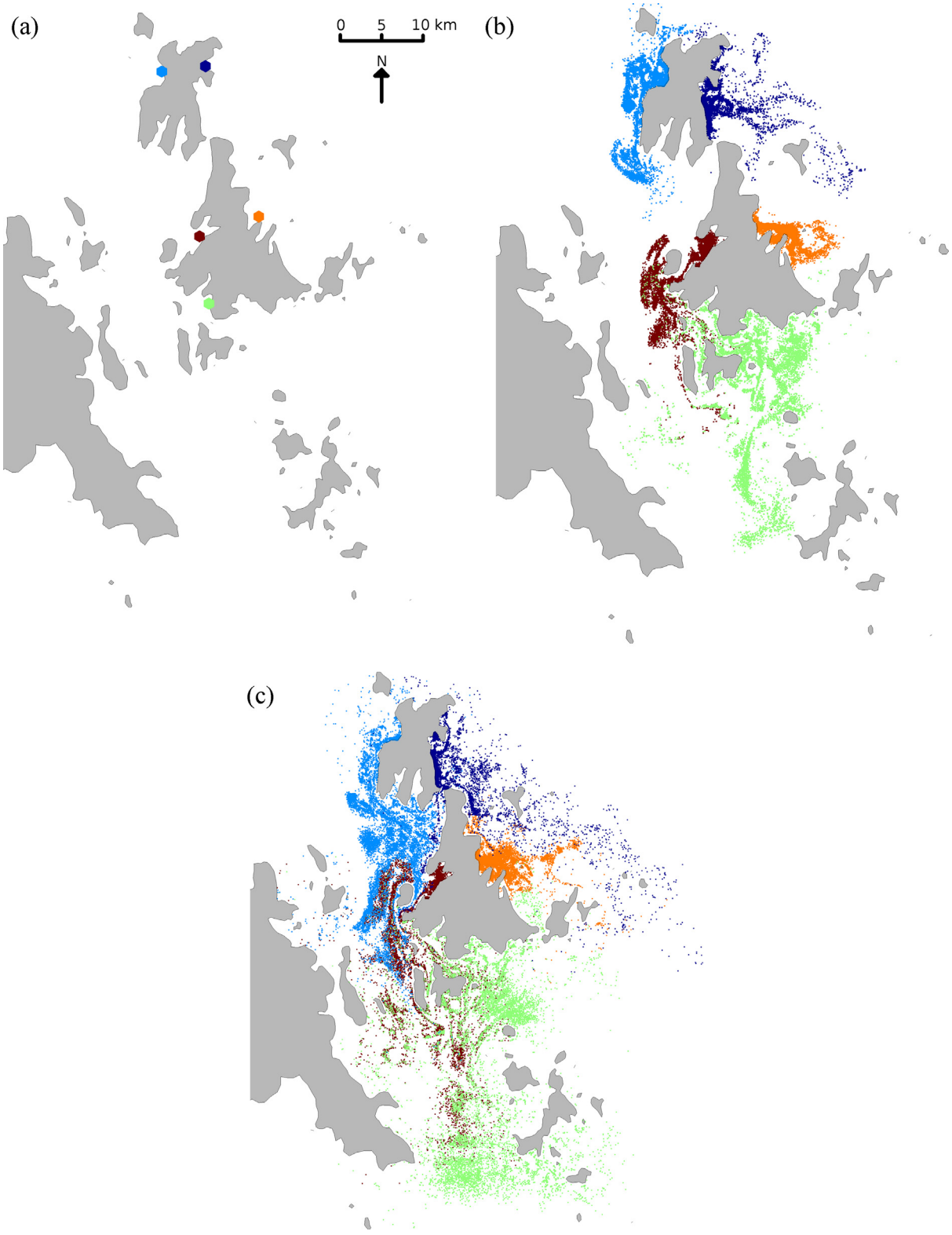

Fig. 9. Images showing the dispersal of particles released at five chosen sites around the Whitsunday Islands over a week. Particles are colour-coded by release site. Mortality and settling were ignored. (a) Initial particle positions. (b) Positions after 3.5 days. (c) Positions after 7 days.

to some extent by a lack of biological data. Finally more work is needed to find a way to achieve an "optimal" MPA spacing which accounts for the different connectivity characteristics of many different species.

Acknowledgements

This work was carried out under the auspices of ARC grant 10/15-028 of the *Communauté française de Belgique*, "Taking up

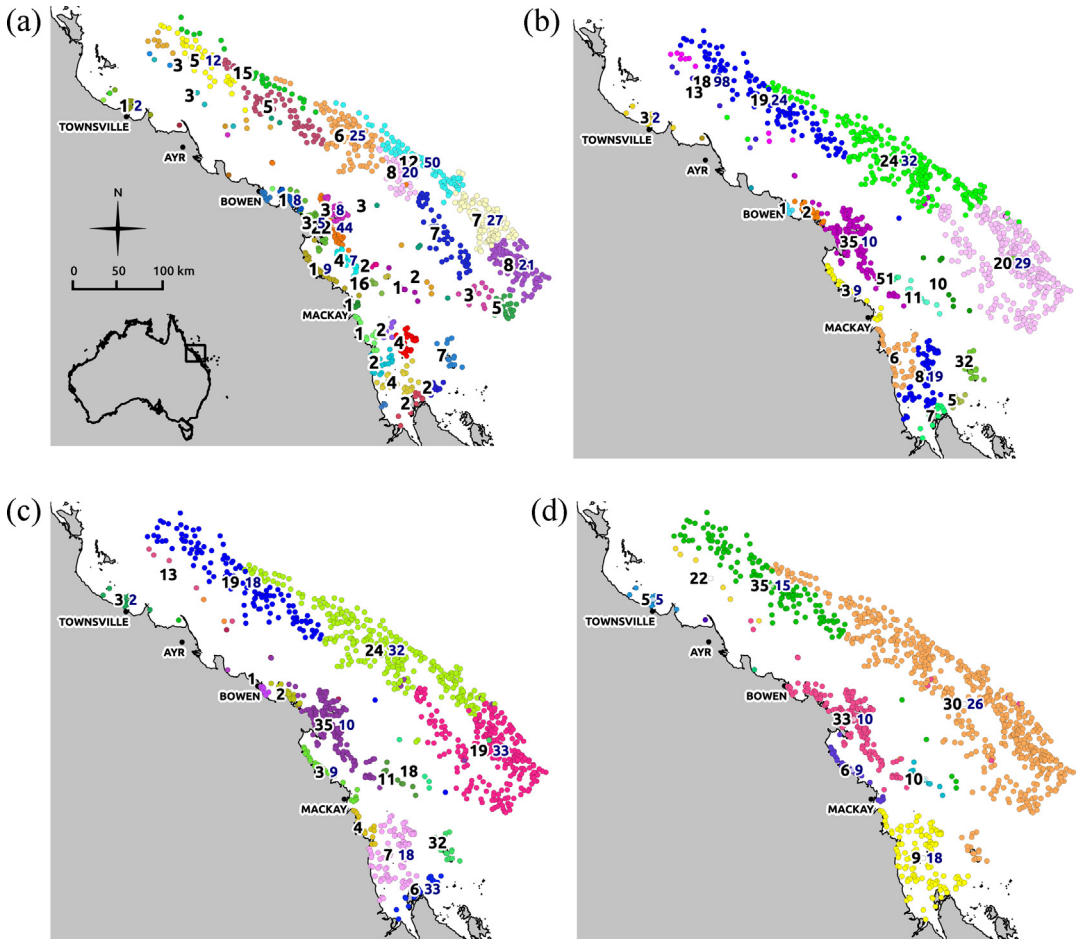

Fig. 10. Equivalent reef community configurations for 4 species of coral larvae. Reefs of the same colour belong to the same community. Black numbers show the weighted connectivity length (km) for reefs in each community. Blue numbers show the average MPA spacing (km) in communities containing more than one MPA. The proportion of connectivity crossing community boundaries is approximately 4% for all configurations, so they are directly comparable with each other. (a) *G. retiformis*. (b) *A. gemmifera*. (c) *P. daedalea*. (d) *A. millepora*. (For interpretation of the references to color in this figure legend, the reader is referred to the web version of the article.)

the challenges of multi-scale marine modelling". Computational resources were provided by the *Centre de Calcul Intensif et Stockage de Masse* (CISM) at the Université catholique de Louvain and the *Consortium des Équipements de Calcul Intensif en Fédération Wallonie Bruxelles* (CÉCI). J. Lambrechts is a post-doctoral researcher with the Belgian Fund for Scientific Research (FNRS). C.J. Thomas thanks Benjamin de Brye, Bruno Seny and Tuomas Kärnä for constructive discussions.

Appendix A. Validation of hydrodynamics

It is known that reef-scale eddies in the wakes of islands in the GBR have a three-dimensional structure with localised upwelling and downwelling (see e.g. Deleersnijder et al., 1992; White and Deleersnijder, 2007), which raises the question of whether a depth-integrated model is sufficient to model circulation in the region. The relatively shallow coastal waters of the GBR have, however, been shown to be generally well-mixed throughout the year, and flow on the continental shelf is known to be primarily horizontal (Middleton and Cunningham, 1984; Wolanski, 1994). Several studies have shown that two-dimensional models can predict physically accurate horizontal currents, even for tidal circulation around islands and headland eddies (e.g. Falconer et al., 1986), as well as for large-scale flow in parts of the GBR (Luick et al., 2007). More specifically Lambrechts et al. (2008) found that the horizontal flow around islands in the GBR simulated using the depth-integrated SLIM model compared favourably to a high-resolution full three-dimensional model validated with observed data. Given the shallow depth and complex topography of the GBR shelf, as well as the well-mixed nature of GBR shelf waters, we therefore argue that it is more useful to achieve reef-scale resolution in the horizontal plane than it is to resolve vertical variations which, in most cases, are relatively small.

The work carried out by Lambrechts et al. (2008) shows that the hydrodynamic model used is able to reproduce small-scale circulation features well, however, it is also necessary to validate the model's ability to realistically reproduce large-scale circulation through the region. This was done by comparing predictions of sea surface elevation (SSE) and water currents with observed data at various mooring sites. Data from long-term moorings obtained from the Integrated Marine Observing System's (IMOS) Great Barrier Reef Ocean Observing System (GBROOS) program run by AIMS/CSIRO were used to validate SSE, whilst current meter data from a variety of sources were used to validate water currents. The locations of the mooring points used are shown in Fig. 1. The SSE observed at different GBROOS mooring sites is shown alongside model predictions for a typical weekly period in Fig. 11. There is a good agreement between the two datasets both in terms of amplitude and phase.

Table 2 shows average longshore current velocities for the different mooring sites compared with model predictions. It should be considered that comparing currents at a given point is very delicate, as any discrepancy in spatial position and water depth can lead to a relatively large change in the observed current, especially

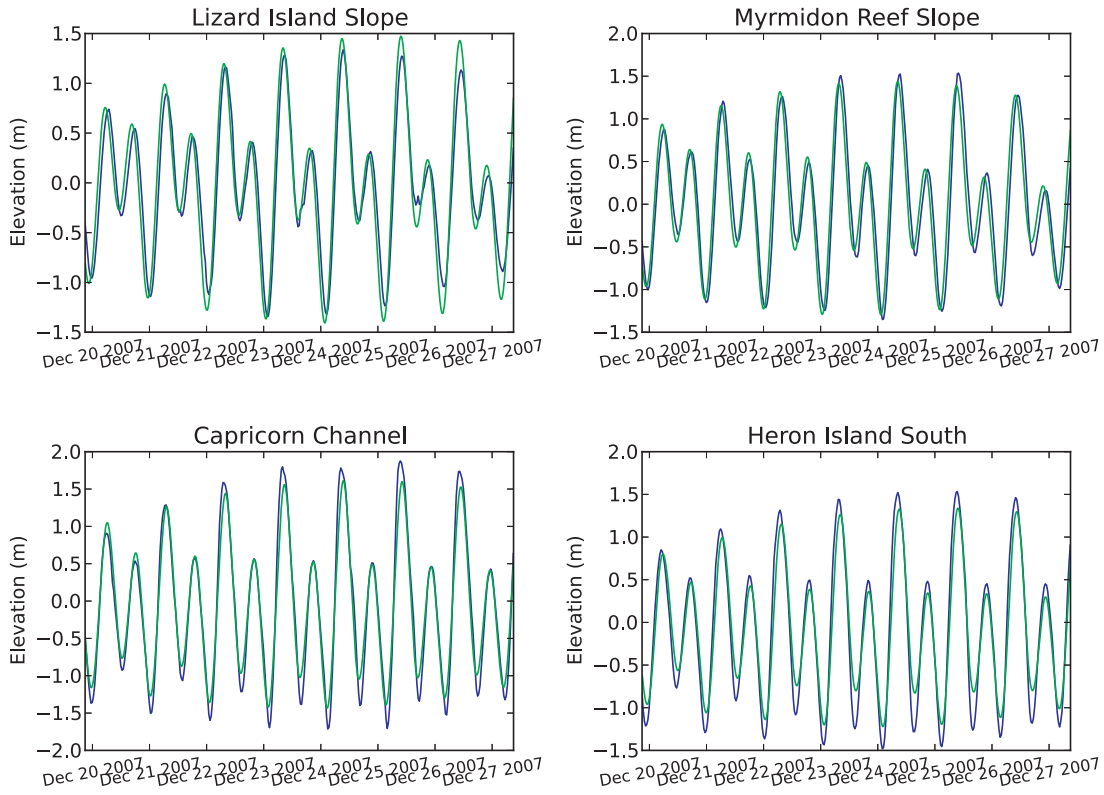

Fig. 11. Graphs showing time-series of elevations at 4 different sites in the model domain. The blue curve shows observed data from the GBROOS mooring network and the green curve shows the model's predictions. The locations of the GBROOS moorings are shown in Fig. 1. (For interpretation of the references to color in this figure legend, the reader is referred to the web version of the article.)

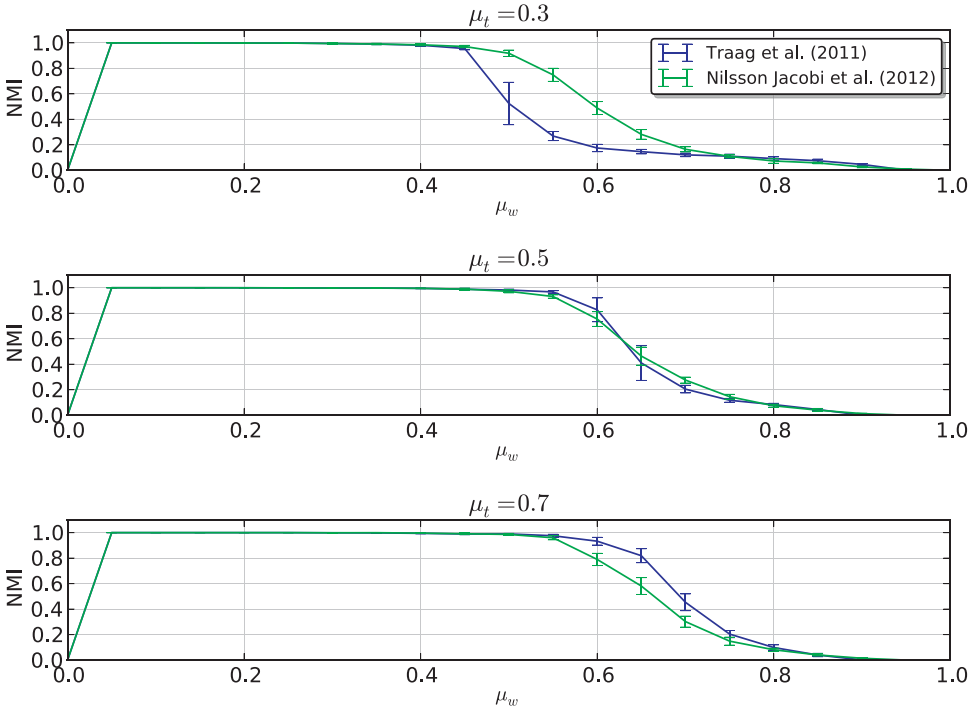

Fig. 12. Results of the tests of the algorithm benchmark tests. Higher values of NMI indicate better performance. Error bars show standard deviation of NMI across repeated runs at the same value of μ_w.

Table 2
Observed longshore residual currents (U_O) and simulated longshore residual currents (U_{SLIM}), in m s^{-1} at various sites in the GBR. Positive indicates a northerly longshore direction, whereas negative indicates a southerly longshore direction. The Source column gives the source of U_O. Locations of moorings shown in Fig. 1. *Sources*: A: Brinkman et al. (2001), B: Andutta et al. (2012), C: Wolanski et al. (1989), D: Middleton and Cunningham (1984)

Site	Latitude (° S)	Longitude (° E)	U_{SLIM}	U_O	Source
Lizard Island	14.7406	145.4253	0.05	0.05	A
Cape Upstart	19.6253	147.9142	−0.04	−0.11	A
Old Reef	19.4071	148.0197	−0.14	−0.10	B
Bowden Reef	19.0600	147.9597	0.00	−0.02	C
Rattray Island	19.9826	148.5833	−0.03	−0.08	B
Hook	19.9400	149.1100	−0.14	−0.15	D
Bushy	20.8900	150.1600	−0.11	−0.13	D
Bell	21.8200	151.1400	−0.04	−0.06	D

close to reefs and islands – which is where most observing stations are situated – as the horizontal shear is often significant in these areas. In this context, Table 2 shows that there is a relatively good agreement between the model predictions and the observed dataset. We can therefore be relatively confident in the ability of the ocean model to realistically reproduce currents and SSE in the domain.

Appendix B. Comparison of two CPM community detection algorithms

We compared the performance of the community detection algorithm employed in this study (described in Traag et al., 2011) with the one used by Nilsson Jacobi et al. (2012), in order to test the validity of using either approach. We used two methods: first we compared the performance of each algorithm in partitioning a standard benchmark network with a known solution, and then we compared the partitions generated by each method for an actual GBR connectivity network.

B.1. Benchmark networks

The standard benchmark networks used were those described in Lancichinetti et al. (2008) and Lancichinetti and Fortunato (2009). We generated directed, weighted benchmark networks and measured the performance of both algorithms in identifying the correct partitions for a range of values of weight and topology mixing parameters (μ_w and μ_t, respectively). The resolution parameter used to partition each network (labelled as γ in Traag et al., 2011 and $1/\beta$ in Nilsson Jacobi et al., 2012) was calculated as the geometric mean of p_{in} and p_{out}, i.e. $\sqrt{p_{in}p_{out}}$, using the notation and definitions from Lancichinetti and Fortunato (2009), and following the same approach as Traag et al. (2011). Ten different networks were generated for each combination of μ_w and μ_t, and the two algorithms were in turn applied to partition each network. The quality of these partitions was measured by calculating the normalised mutual information (NMI) between these partitions and the true partitions for the network. NMI provides a measure of how similar two sets of partitions are. An average value of NMI was calculated for each combination of μ_w and μ_t, along with its standard deviation.

Table 3
Comparison of Traag et al. (2011) and Nilsson Jacobi et al. (2012) community detection methods for *G. retiformis* connectivity networks at low, medium and high values of γ. Each algorithm was run 10 times and average values are shown.

γ	NMI	Number of communities	
		Traag et al. (2011)	Nilsson Jacobi et al. (2012)
0.0004	0.90	44	42
0.00003	0.79	17	15
0.000006	0.87	11	9

The results of the comparison are shown in Fig. 12, where the x-axis spans a range of values of μ_w, and the y-axis shows NMI. The higher the NMI, the better the quality of the partitions found by the algorithm. These results show that both methods performed well, though the method of Nilsson Jacobi et al. (2012) worked better for networks with lower values of μ_t, whilst the method of Traag et al. (2011) worked marginally better for networks with higher values of μ_t.

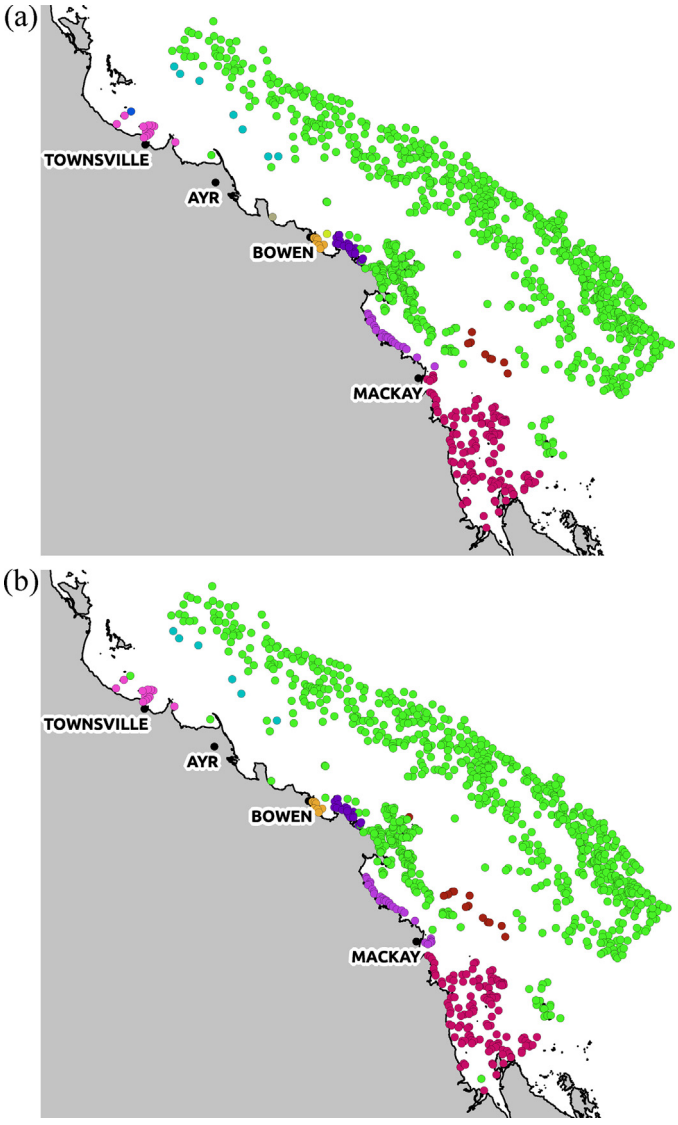

Fig. 13. Partitioning configurations generated for low-γ *G. retiformis* network obtained using different community detection algorithms. (a) Method of Traag et al. (2011). (b) Method of Nilsson Jacobi et al. (2012).

B.2. GBR network

Both community detection methods were then used to partition the set of GBR connectivity networks discussed in Section 3.2. Table 3 shows the number of communities identified by each method for each network, as well as the NMI between the two partitions. These indicate that the high- and low-γ networks match well, whilst the middle-γ network has a slightly lower NMI. The differences between the partitions created by the two algorithms are generally limited to reefs close to the boundaries of communities being placed in one or the other neighbouring community. Fig. 13 compares typical partitioning configurations generated by each algorithm for the low-γ case. Overall, the communities identified were not very sensitive to the community detection method used.

References

Almany, G.R., Connolly, S.R., Heath, D.D., Hogan, J.D., Jones, G.P., McCook, L.J., Mills, M., Pressey, R.L., Williamson, D.H., 2009. Connectivity, biodiversity conservation and the design of marine reserve networks for coral reefs. Coral Reefs 28, 339–351.

Andutta, F.P., Ridd, P.V., Wolanski, E., 2011. Dynamics of hypersaline coastal waters in the Great Barrier Reef. Estuarine, Coastal and Shelf Science 94, 299–305.

Andutta, F.P., Kingsford, M.J., Wolanski, E., 2012. 'Sticky water' enables the retention of larvae in a reef mosaic. Estuarine, Coastal and Shelf Science 54, 655–668.

Beaman, R.J., 2010. Project 3DGBR: A High-Resolution Depth Model for the Great Barrier Reef and Coral Sea. Final Report Project 2.5i.1a, Marine and Tropical Sciences Research Facility (MTSRF), Cairns, Australia.

Blondel, V.D., Guillaume, J-.L., Lambiotte, R., Lefebvre, E., 2008. Fast unfolding of communities in large networks. Journal of Statistical Mechanics: Thoery and Experiment 10, P10008.

Brinkman, R., Wolanski, E., Deleersnijder, E., McAllister, F., Skirving, W., 2001. Oceanic inflow from the Coral Sea into the Great Barrier Reef. Estuarine, Coastal and Shelf Science 54, 655–668.

Buston, P.M., Jones, G.P., Planes, S., Thorrold, S.R., 2012. Probability of successful larval dispersal declines fivefold over 1 km in a coral reef fish. Proceedings of the Royal Society B 279, 1883–1888.

Connolly, S.H., Baird, A.R., 2010. Estimating dispersal potential for marine larvae: dynamic models applied to scleractinian corals. Ecology 91 (12), 3572–3583.

Cowen, R.K., Sponaugle, S., 2009. Larval dispersal and marine population connectivity. Annual Review of Marine Science 1, 443–466.

Cowen, R.K., Paris, C.B., Srinivasan, A., 2006. Scaling of connectivity in marine populations. Science 311, 522–527.

de Brauwere, A., de Brye, B., Blaise, S., Deleersnijder, E., 2011. Residence time, exposure time and connectivity in the Scheldt estuary. Journal of Marine Systems 84 (3/4), 85–95.

de Brye, Benjamin, Anouk de Brauwere, Olivier Gourgue, Tuomas Karna, Jonathan Lambrechts, Richard Comblen, Eric Deleersnijder, 2010. A finiteelement: multiscale model of the scheldt tributaries, river, estuary and rofi. Coastal Engineering 57 (9), 850–863.

Deleersnijder, E., Norro, A., Wolanski, E., 1992. A three-dimensional model of the water circulation around an island in shallow water. Continental Shelf Research 12 (7/8), 891–906.

Drew, J.A., Barber, P.H., 2012. Comparative phylogeography in Fijian coral reef fishes: a multi-taxa approach towards marine reserve design. PLoS ONE 7 (10).

Egbert, G.D., Erofeeva, S.Y., 2002. Efficient inverse modeling of barotropic ocean tides. Journal of Atmospheric and Oceanic Technology 19, 183–204.

Falconer, R., Wolanski, E., Mardapitta-Hadjipandeli, L., 1986. Modeling tidal circulation in an island's wake. Journal of Waterway, Port, Coastal, and Ocean Engineering 112, 234–254.

Fisher, R., Bellwood, D.R., 2003. Undisturbed swimming behaviour and nocturnal activity of coral reef fish larvae. Marine Ecology Progress Series 263, 177–188.

Fortunato, S., 2007. Resolution limit in Community Detection. Proceedings of the National Academy of Sciences 104, 36–41.

Fortunato, S., 2010. Community detection in graphs. Physics Reports 486, 75–174.

GBRMPA, 2007. Coastal Features within and Adjacent to the Great Barrier Reef World Heritage Area. Technical report, Great Barrier Reef Marine Park Authority, Australia.

Gerlach, G., Atema, J., Kingsford, M.J., Black, K.P., Miller-Sims, V., 2007. Smelling home can prevent dispersal of reef fish larvae. Proceedings of the National Academy of Sciences of the United States of America 104 (3), 858–863.

Grimm, V., Berger, U., Bastiansen, F., Eliassen, S., Ginot, V., Giske, J., Goss-Custard, J., Grand, T., Heinz, S.K., Huse, G., Huth, A., Jepsen, J.U., Jorgensen, C., Mooij, W.M., Muller, B., Pe'er, G., Piou, C., Railsback, S.F., Robbins, A.M., Robbins, M.M., Rossmanith, E., Ruger, N., Strand, E., Souissi, S., Stillman, R.A., Vabo, R., Visser, U., DeAngelis, D.L., 2006. A standard protocol for describing individual-based and agent-based models. Ecological Modelling 198, 115–126.

Guizien, K., Belharet, M., Marsaleix, P., Guarinia, J.M., 2012. Using larval dispersal simulations for marine protected area design. Application to the Gulf of Lions (northwest Mediterranean). Limnology and Oceanography 57 (4), 1099–1112.

Hamann, M., Grech, A., Wolanski, E., Lambrechts, J., 2011. Modelling the fate of marine turtle hatchlings. Ecological Modelling 222, 1515–1521.

Hunter, J.R., Craig, P.D., Phillips, H.E., 1993. On the use of random waml models with spatially variable diffusivity. Journal of Computational Physics 106, 366–376.

Jones, G.P., Almany, G.R., Russ, G.R., Sale, P.F., Steneck, R.S., van Oppen, M.J.H., Willis, B.L., 2009. Larval retention and connectivity among populations of corals and reef fishes: history and advances and challenges. Coral Reefs 28, 307–323.

Kalnay, E., Kanamitsu, M., Kistler, R., Collins, W., Deaven, D., Gandin, L., Iredell, M., Saha, S., White, G., Woollen, J., Zhu, Y., Leetmaa, A., Reynolds, B., Chelliah, M., Ebisuzaki, W., Higgins, W., Janowiak, J., Mo, K.C., Ropelewski, C., Wang, J., Jenne, R., Joseph, D., 1996. The ncep/ncar 40-year reanalysis project. Bulletin of the American Meteorological Society 77, 437–470.

Kininmonth, S., van Oppen, M.J.H., Possingham, H.P., 2010a. Determining the community structure of the coral Seriatopora hystrix from hydrodynamic and genetic networks. Ecological Modelling 221, 2870–2880.

Kininmonth, S.J., De'ath, G., Possingham, H.P., 2010b. Graph theoretic topology of the Great but small Barrier Reef world. Theoretical Ecology 3, 75–88.

Lambrechts, J., Hanert, E., Deleersnijder, E., Bernard, P.-E., Legat, V., Remacle, J.-F., Wolanski, E., 2008. A multi-scale model of the hydrodynamics of the whole Great Barrier Reef. Estuarine, Coastal and Shelf Science 79, 143–151.

Lancichinetti, A., Fortunato, S., 2009. Community detection algorithms: A comparative analysis. Physical Review E 80, 056117.

Lancichinetti, A., Fortunato, S., Radicchi, F., 2008. Benchmark graphs for testing community detection algorithms. Physical Review E 78, 46110.

Largier, J.L., 2003. Considerations in estimating larval dispersal distances from oceanographic data. Ecological Applications 13, S71–S89.

Legrand, S., Deleersnijder, E., Hanert, E., Legat, V., Wolanski, E., Highresolution, 2006. unstructured meshes for hydrodynamic models of the Great Barrier Reef, Australia. Estuarine, Coastal and Shelf Science 68, 36–46.

Leis, J.M., Van Herwerden, L., Patterson, H.M., 2011. Estimating connectivity in marine fish populations: what works best. Oceanography and Marine Biology: An Annual Review 49, 193–234.

Luick, J.L., Mason, L., Hardy, T., Furnas, M.J., 2007. Circulation in the Great Barrier Reef lagoon using numerical tracers and in situ data. Continental Shelf Research 27, 757–778.

Middleton, J.H., Cunningham, A., 1984. Wind-forced continental shelf waves from a geographical origin. Continental Shelf Research 3 (3), 215–232.

Mumby, P.J., Elliott, I.A., Eakin, M., Skirving, W., Paris, C.B., Edwards, H.J., Enriquez, S., Iglesias-Prieto, R., Cherubin, L.M., Stevens, J.R., 2011. Reserve design for uncertain responses of coral reefs to climate change. Ecology Letters 14, 132–140.

Munday, P.L., Leis, J.M., Lough, J.M., Paris, C.B., Kingsford, M.J., Berumen, M.L., Lambrechts, J., 2009. Climate change and coral reef connectivity. Coral Reefs 28, 379–395.

Newman, M.E.J., Girvan, M., 2004. Finding and evaluating community structure in networks. Physical Review E 69, 026113.

Nilsson Jacobi, M., Andre, C., Doos, K., Jonsson, P.R., 2012. Identification of subpopulations from connectivity matrices. Physical Review E 69, 026113.

Okubo, A., 1971. Oceanic diffusion diagrams. Deep Sea Research 18, 789–802.

Olds, A.D., Connolly, R.M., Pitt, K.A., Maxwell, P.S., 2012. Habitat connectivity improves reserve performance. Conservation Letters 5, 56–63.

Palumbi, S.R., 2003. Population genetics and demographic connectivity and and the design of marine reserves. Ecological Applications 13, S146–S158.

Paris, C.B., Cherubin, L.M., Cowen, R.K., 2007. Surfing and spinning and or diving from reef to reef: effects on population connectivity. Marine Ecology Progress Series 347, 285–300.

Proulx, S.R., Promislow, D.E.L., Phillips, P.C., 2005. Network thinking in ecology and evolution. Trends in Ecology and Evolution 20 (6), 345–353.

Ronhovde, P., Nussinov, Z., 2010. Local resolution-limit-free Potts model for community detection. Physical Review E 81, 046114.

Sassi, M.G., Hoitink, A.J.F., De Brye, B., Vermeulen, B., Deleersnijder, E., 2011. Tidal impact on the division of river discharge over distributary channels in the Mahakam Delta. Ocean Dynamics 61, 2211–2228.

Smith, S.D., Banke, E.G., 1975. Variation of the sea surface drag coefficient with wind speed. Quarterly Journal of the Royal Meteorological Society 101, 665–673.

Spagnol, S., Wolanski, E., Deleersnijder, E., Brinkman, R., McAllister, F., Cushman-Roisin, B., Hanert, E., 2001. An error frequently made in the evaluation of advective transport in two-dimensional Lagrangian models of advection-diffusion in coral reef waters. Marine Ecology Progress Series 235, 299–302.

Traag, V.A., Van Dooren, P., Nesterov, Y., 2011. Narrow scope for resolution limit-free community detection. Physical Review E 84, 016114.

Treml, E., Halpin, P., Urban, D., Pratson, L., 2008. Modeling population connectivity by ocean currents, a graph-theoretic approach for marine conservation. Landscape Ecology 23, 19–36.

Vermeij, M.J.A., Marhaver, K.L., Huijbers, C.M., Nagelkerken, I., Simpson, S.D., 2010. Coral larvae move toward reef sounds. PLoS ONE 5 (5).

Werner, F., Cowen, R., Paris, C.B., 2007. Coupled biological and physical models: present capabilities and necessary developments for future studies of population connectivity. Oceanography 20, 54–69.

White, L., Deleersnijder, E., 2007. Diagnoses of vertical transport in a three-dimensional finite element model of the tidal circulation around an island. Estuarine, Coastal and Shelf Science 74, 655–669.

Wolanski, E., 1994. Physical Oceanographic Processes of the Great Barrier Reef. CRC Press, Boca Raton, FL.
Wolanski, E., Spagnol, S., 2000. Sticky waters in the Great Barrier Reef. Estuarine, Coastal and Shelf Science 50, 27–32.
Wolanski, E., Burrage, D., King, B., 1989. Trapping and diffusion of coral eggs near Bowden Reef, Great Barrier Reef following mass coral spawning. Continental Shelf Research 9, 479–496.
Wolanski, E., Brinkman, R., Spagnol, S., McAllister, F., Steinberg, C., Skirving, W., Deleersnijder, E., 2003. Chapter 15 – merging scales in models of water circulation: perspectives from the Great Barrier Reef. In: Lakhan, V.C. (Ed.), Advances in Coastal Modeling, vol. 67 of Elsevier Oceanography Series. Elsevier, pp. 411–429.
Wolanski, E., Lambrechts, J., Thomas, C., Deleersnijder, E., 2013. The net water circulation through Torres strait. Continental Shelf Research 64, 66–74.